Fluctuations with Cubic Symmetry in a Hexagonal Copolymer Microstructure

Chang Yeol Ryu,[1] Martin E. Vigild,[1] and Timothy P. Lodge[2]
[1]*Department of Chemical Engineering & Materials Science, University of Minnesota, Minneapolis, Minnesota 55455-0431*
[2]*Department of Chemistry, University of Minnesota, Minneapolis, Minnesota 55455-0431*
(Received 24 June 1998)

A triblock copolymer that undergoes a thermotropic order-order transition between hexagonally packed cylinders (C) and body-centered-cubic spheres (S) is examined. Transmission electron microscopy provides real space images, and small-angle x-ray scattering the reciprocal space signature, of fluctuations with cubic symmetry in the stable (shear-aligned) hexagonal phase. These results support recent theoretical predictions. There is evidence of an interesting induction time for the onset of fluctuations that is attributed to a slight mismatch in principal lattice spacings between the C and S microstructures. [S0031-9007(98)07903-4]

PACS numbers: 64.70.–p, 61.25.Hq, 61.50.Ks, 64.70.Ja

Block copolymers as a class of amphiphilic molecules exhibit a rich variety of equilibrium microstructures that are accessible by both thermotropic and lyotropic order-disorder and order-order transitions [1,2]. As is typical in soft materials, these phase transitions are dictated by complex energetic and entropic contributions to the free energy, and are often presaged by fluctuations of substantial amplitude [3,4]. Interesting issues of nucleation, metastability, stability, and kinetic pathways arise naturally in such systems. For block copolymers the natural length scale associated with the various mesophases is set by the molecular size (i.e., 10–100 nm), and is thus conveniently located for analysis by small-angle scattering and electron microscopy. Furthermore, sluggish molecular rearrangements in the bulk enable straightforward examination of structural evolution by rheological techniques. The combination of scattering, microscopy, and rheology affords a powerful means to examine copolymer phase transitions in detail.

Of particular interest are thermotropic order-order transitions (OOT) between microphases of different symmetry, such as the cylinder to sphere ($C \rightarrow S$) transition. The existence of a thermally reversible transition between a hexagonal array of rods (space group $p6m$) and a body-centered cubic (bcc) array of spheres ($Im\bar{3}m$) for asymmetric block copolymers was anticipated by mean-field theory [5], and has been established experimentally [6–8]. Furthermore, an epitaxial relationship between the $\langle 001 \rangle$ axis of C and the $\langle 111 \rangle$ axis of S was demonstrated [6,7]. Recent theoretical examination of pathways for the $C \rightarrow S$ transition predicts that the morphology evolves through periodic (peristaltic) undulations in the cylinder diameters with bcc symmetry [9–14]; such undulations have been invoked to explain certain features of the experimental work [6,8]. In this Letter we provide the first direct microscopic evidence of fluctuations with cubic symmetry in the stable C phase. We also locate the thermodynamic equilibrium (coexistence) transition temperature T_{OOT} and obtain estimates of the temperatures representing the stability limits for the C and S phases, T_s^C and T_s^S, respectively.

Two groups have calculated the relative stability or metastability of the various microphases observed in the weak and intermediate segregation regime, and the kinetic pathways between them. Laradji *et al.* [9,10] applied a theory for anisotropic fluctuations developed by Shi *et al.* [11] to locate spinodal lines for each ordered phase, and the most unstable fluctuation modes. These were then used to infer the most probable route for a given order-order transition. Qi and Wang employed a time-dependent Ginzburg-Landau approach to follow structural evolution after a (temperature) jump into a different phase [12–14]. For the particular case of the $C \rightarrow S$ transition, and the identity of the least stable fluctuation mode, the results of the two approaches are similar. Figure 1(a) provides a real space representation of this mode following Laradji *et al.* [9], whereas Fig. 1(b) shows the reciprocal space picture as proposed by Qi and Wang [12]. In the latter, the cylinders are oriented along $\mathbf{x}$, the two sets of six large black dots represent the Bragg reflections at $q_x = 0$ on the surfaces of the $|\mathbf{q}| = |\mathbf{q}^*|$ and $|\mathbf{q}| = |\sqrt{3}\,\mathbf{q}^*|$ spheres in reciprocal space, and the dashed rings represent the fluctuation modes associated with q^*. Where two rings intersect there are 12 small gray dots, which correspond to the expected fluctuation peaks; the total of 18 dots on the $|\mathbf{q}| = |\mathbf{q}^*|$ sphere represent the reciprocal lattice for a twinned bcc structure [12].

We examined a poly(styrene-*b*-isoprene-*b*-styrene) triblock copolymer, with block molecular weights of 1×10^4, 1×10^5, and 1×10^4, respectively, and a polydispersity index less than 1.06. Application of large amplitude reciprocating shear produced a specimen with a high degree of uniaxial cylinder orientation [8]. A portion of the oriented specimen was placed in the rheometer in order to monitor the low frequency dynamic shear elastic modulus parallel to the cylinder axis, $G'_{\parallel}$, under small amplitude oscillatory shear. The results for three different heating/cooling rates are shown as a function of temperature in Fig. 2(a). For the trace obtained at ± 0.3 °C/min, the $C \rightarrow S$ transition that begins near 198 °C upon heating, and the $S \rightarrow C$ transition near 190 °C upon cooling,

 0031-9007/98/81(24)/5354(4)$15.00

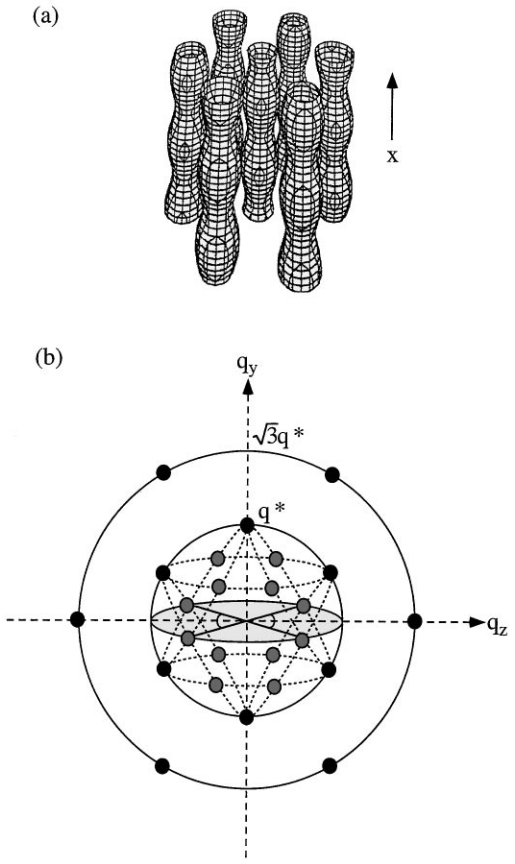

FIG. 1. Dominant fluctuation modes in a hexagonal block copolymer: (a) Real space image, following Laradji *et al.* [9] and (b) reciprocal space image, following Qi and Wang [12]. The angle indicated in the shaded q_x-q_z plane is 110°.

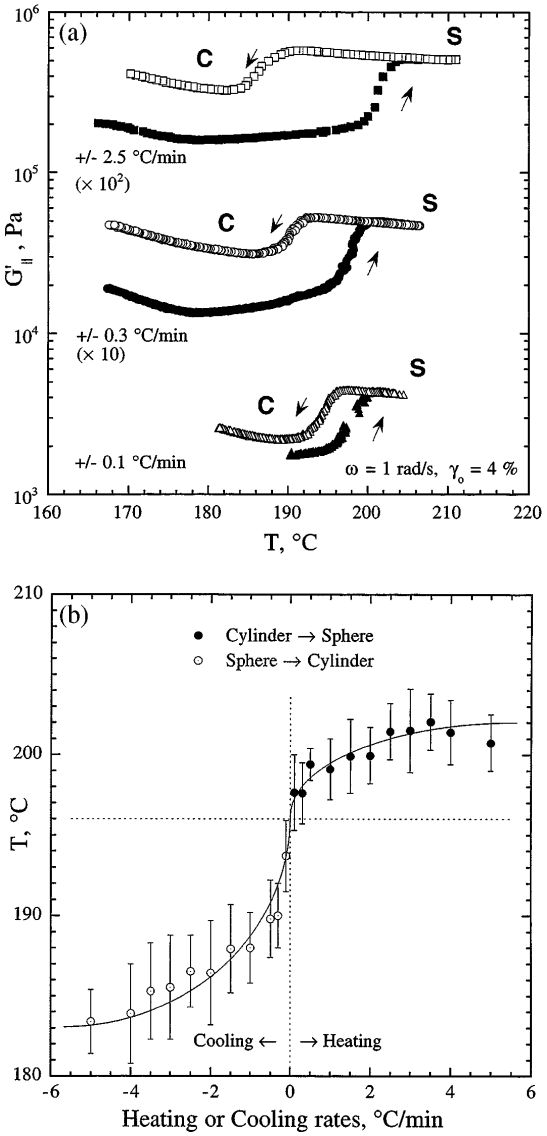

FIG. 2. (a) Rheological hysteresis loops for the $C \rightarrow S$ and $S \rightarrow C$ transitions, at three different heating and cooling rates, and (b) the resulting transition temperatures; the error bars indicate the onset and completion of the sharp rise or drop in $G'_{\parallel}$. The smooth curve in (b) is a guide to the eye.

are indicated by a sharp break in the modulus (all assignments were confirmed by x-ray scattering). (In contrast, $G'_{\perp}$ is an order of magnitude larger than $G'_{\parallel}$, and actually drops during the $C \rightarrow S$ transition, as shown elsewhere [8].) The key feature in Fig. 2(a) is the gradual increase in $G'_{\parallel}$ with T that begins near 178 °C and extends up to the sharp $C \rightarrow S$ transition. This increase was previously postulated to result from undulations in the cylinder diameter, which act to increase resistance to the relative axial motion of neighboring cylinders [8]; here we confirm this assignment.

Two alternative hypotheses bear consideration. One is that the sharp feature near 200 °C is actually the stability limit of C, and that the change in slope of $G'_{\parallel}(T)$ near 178 °C reflects the onset of slow nucleation of S. The other is that this temperature interval represents a broad region of C and S coexistence, due to polydispersity in molecular weight and/or heterogeneity in composition. However, both of these explanations may be discounted, based in large part on the results in Figs. 2(a) and 2(b). The presence of a distinct hysteresis loop is apparent, which narrows considerably upon decreasing $|\partial T/\partial t|$; the sharp break in $G'_{\parallel}$ is consistently observed, but occurs at a rate-dependent temperature. In Fig. 2(b) the transition temperature is plotted as a function of the heating/cooling rate, with the error bars indicating the range of temperature from the onset of the abrupt increase in $G'_{\parallel}$ to the attainment of the S plateau. From these results T_{OOT} is determined to be 196 ± 1 °C. The stability limit of C, T_s^C, is estimated to be 202 ± 2 °C, and that of S, $T_s^S \approx 183 \pm 3$ °C. The former is more precisely determined, because the transition temperature is independent of further increases in heating rate. Heat transfer limitations in the rheometer preclude reliable measurements at larger heating or cooling rates (and care was taken to calibrate the actual sample temperature versus the nominal "rheometer temperature" for the different rates). Theory anticipates that T_s^S is farther from T_{OOT}

than T_s^C, in agreement with these data, due to the barrier to the coalescence of two spherical micelles [9]. Chromatography confirmed that the samples did not suffer significant degradation at the elevated temperatures employed in rheology or small-angle x-ray scattering (SAXS).

Transmission electron micrographs of the shear-oriented material were taken after annealing for a few minutes at various temperatures, followed by rapid quenching into ice water. Specimens were then cryomicrotomed at $-110\,^{\circ}\mathrm{C}$ to provide about 70 nm thick films, which were stained by exposure to the vapor above a 4% OsO_4 aqueous solution. Figures 3(a)–3(d) show the results obtained, in order of increasing annealing temperature. Figure 3(a) shows aligned cylinders annealed at 173 °C, a temperature below the change in $\partial G'_{\|}/\partial T$. Although some defects and wiggles in cylinder orientation are visible, the stable, highly oriented cylinder structure is apparent. In Fig. 3(b), annealed for 10 min at 183 °C, there is clear evidence of a systematic distortion in the individual cylinders, particularly in a "grain" approximately 0.5 μm in extent. Close examination suggests a locally approximately hexagonal arrangement of elongated "droplets," with the underlying cylindrical orientation preserved. Similar submicron grains were routinely observed in specimens annealed at 183 °C. After annealing for 10 min at 193 °C, 3 °C below T_{OOT}, the sample acquires a similar mottled pattern, but which now extends throughout the field of view [Fig. 3(c)]; again the initial cylinder orientation is still apparent. The

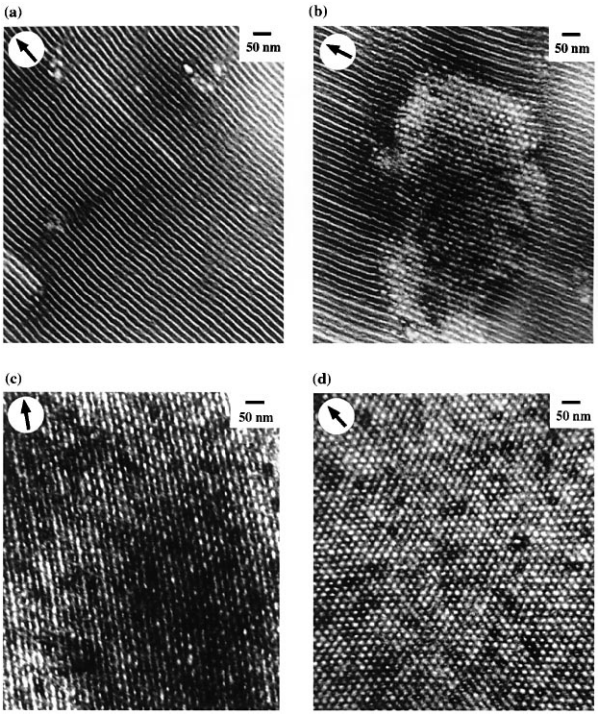

FIG. 3. Representative transmission electron micrographs after annealing (a) at 173 °C; (b) for 10 min at 183 °C; (c) for 10 min at 193 °C; (d) for 5 min at 210 °C. The shear direction (**x**) is indicated by the arrow in each image.

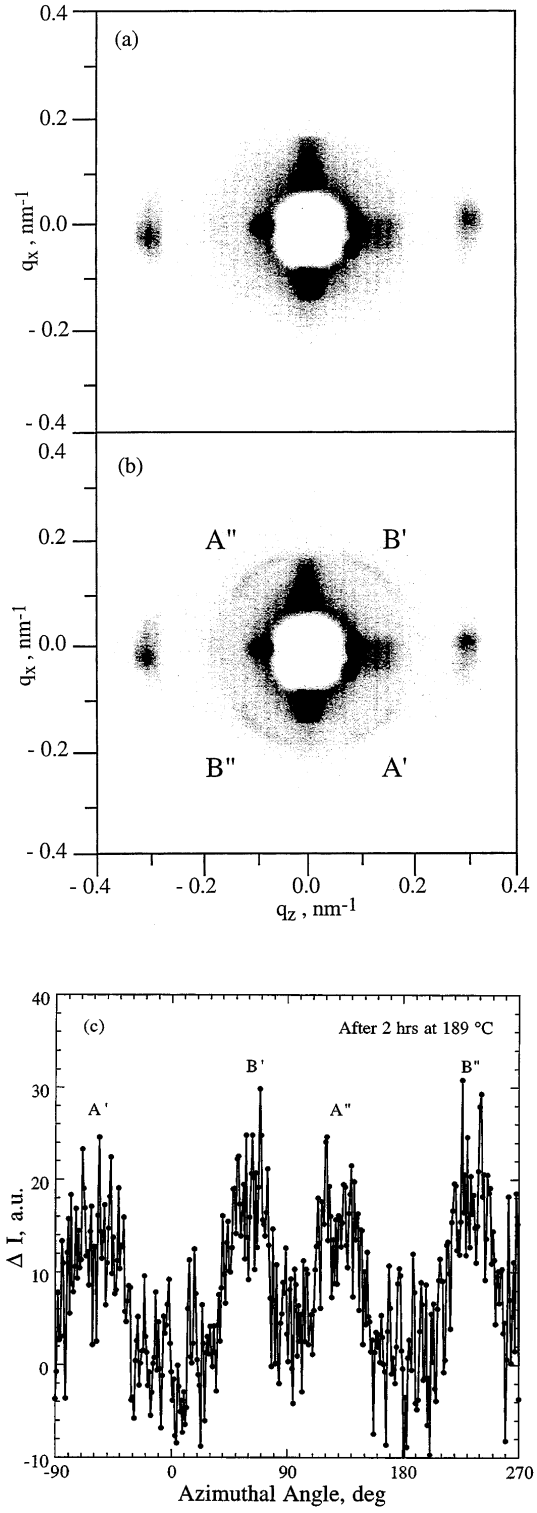

FIG. 4. SAXS patterns for a shear-oriented specimen: (a) After annealing for 1 h at 189 °C, with the two peaks corresponding to $\pm\sqrt{3}\,q^*$; (b) after annealing for 2 h at 189 °C, with the fluctuation peaks designated A', A'', B', and B''; (c) azimuthal plot at $q = q^*$ for the data in (b), after subtraction of the data in (a) as background. The four lobes of intensity around the beamstop are parasitic scattering.

(100) plane of cylinders will, after epitaxial transformation, become the (110) plane of the bcc lattice. However, as the $\langle 001 \rangle$ axis of C becomes the $\langle 111 \rangle$ axis of S two equivalent bcc orientations are possible, leading to a twinned structure in a macroscopic sample. Each twin should exhibit a distorted hexagonal array of spheres in the (100) cylinder plane, which is consistent with the image in Fig. 3(c). In Fig. 3(d), a specimen annealed for 5 min at 210 °C is shown, with the image corresponding to the (110) plane of a well-developed bcc structure. The arrow indicates a $\langle 111 \rangle$ axis.

Although the TEM images provide strong evidence for the superposition of cubic fluctuations on the cylindrical structure, the final test requires the appropriate SAXS signature. A well-oriented specimen confined between Kapton sheets was placed in the sample chamber at room temperature, with the cylinder axis oriented approximately vertically [**x** in Fig. 1(b)] and the x rays incident along **y**. Therefore SAXS patterns were observed in the q_x-q_z plane [shaded area in Fig. 1(b)]. The sample was heated to 189 °C at 1 °C/min, and then annealed for 1 h. The resulting scattering pattern (20 min exposure) is shown in Fig. 4(a); there are distinct Bragg peaks at $\pm\sqrt{3}\,q^*$, and parasitic scattering in four lobes around the beamstop, but there is no scattering at q^*. After a further hour of annealing, a 20 min exposure produced the pattern in Fig. 4(b). According to Fig. 1(b), the weak fluctuation peaks should appear on the q^* ring, with an angle of 110° between them. These fluctuation peaks (denoted A', A'' and B', B'') are clearly evident in Fig. 4(b), although smeared azimuthally around the ring at q^*. The scattering in Fig. 4(a) was subtracted from that in Fig. 4(b), and then the intensity integrated for a small interval around q^*. The resulting azimuthal plot of the intensity difference is shown in Fig. 4(c), with the A', A'', B', and B'' peaks indicated. The peaks are well resolved, and are separated by an angle that is the expected 110° within the uncertainty. This result confirms the existence of bcc fluctuations superposed on the hexagonal lattice, as anticipated by theory [12].

One additional feature of these results deserves comment. We consistently observed an induction period, about 1 h in the case of Fig. 4, before the SAXS signature of fluctuations is cleanly resolved; this is suggestive of a nucleated process. Similarly, the TEM image in Fig. 3(b) shows a distinct boundary between fluctuating and nonfluctuating regions. This is counter to standard thermally induced order-parameter fluctuations, which arise spontaneously. We suspect this result is due to a small but distinct mismatch of 3%–4% between q^* of C and S [8], which presents a barrier to the growth of fluctuations, or, more precisely, inhibits the development of long-ranged spatial coherence in the fluctuations. Further annealing leads to a slow increase in scattered intensity in the fluctuation peaks, attributable to the gradual refinement of the fluctuation structure and the attendant disruption of the long-range cylinder alignment. In the rheological measurements, however, there was no such induction period in terms of the response attributed to fluctuations. This raises the intriguing possibility that even the small amplitude strain applied ($\leq 4\%$) is sufficient to overcome the putative "nucleation" barrier for fluctuations. Finally, we note that analogous small-angle scattering evidence of cubic fluctuations on a lamellar mesophase has recently been observed [15], and that all these results are reminiscent of the premartensitic phonon mode softening observed in certain alloys [16].

This work was supported by the National Science Foundation through DMR-9528481 (T. P. L.), the Carlsberg Foundation (M. E. V.), and the Danish Technical Research Council (M. E. V.). Helpful discussions with Z.-G. Wang, K. Almdal, P.-A. Lindgård, and F. S. Bates are appreciated.

[1] F. S. Bates and G. H. Fredrickson, Annu. Rev. Phys. Chem. **41**, 525 (1990).
[2] F. S. Bates, M. F. Schulz, A. K. Khandpur, S. Förster, J. H. Rosedale, K. Almdal, and K. Mortensen, J. Chem. Soc. Faraday Disc. **98**, 7 (1994).
[3] G. Gompper and M. Schick, *Self-Assembling Amphiphilic Systems* (Academic Press, New York, 1994).
[4] W. M. Gelbart, A. Ben-Shaul, and D. Roux, *Micelles, Membranes, Microemulsions, and Monolayers* (Springer, New York, 1994).
[5] L. Leibler, Macromolecules **13**, 1602 (1980).
[6] K. A. Koppi, M. Tirrell, F. S. Bates, K. Almdal, and K. Mortensen, J. Rheol. **38**, 999 (1994).
[7] S. Sakurai, T. Hashimoto, and L. J. Fetters, Macromolecules **29**, 740 (1996).
[8] C. Y. Ryu, M. S. Lee, D. A. Hajduk, and T. P. Lodge, J. Polym. Sci., Polym. Phys. Ed. **35**, 2811 (1997).
[9] M. Laradji, A.-C. Shi, J. Noolandi, and R. C. Desai, Macromolecules **30**, 3242 (1997).
[10] M. Laradji, A.-C. Shi, R. C. Desai, and J. Noolandi, Phys. Rev. Lett. **78**, 2577 (1997).
[11] A.-C. Shi, J. Noolandi, and R. C. Desai, Macromolecules **29**, 6487 (1996).
[12] S. Qi and Z.-G. Wang, Polymer **39**, 4639 (1998).
[13] S. Qi and Z.-G. Wang, Phys. Rev. Lett. **76**, 1679 (1996).
[14] S. Qi and Z.-G. Wang, Phys. Rev. E **55**, 1682 (1997).
[15] K. A. Almdal, M. E. Vigild, and K. Mortensen (unpublished).
[16] U. Stuhr, P. Vorderwisch, V. V. Kokorin, and P.-A. Lindgård, Phys. Rev. B **56**, 14 360 (1997).